Colloid Polym Sci (2005) 283: 854–861
DOI 10.1007/s00396-004-1227-8

Rodrigo A. Segura
Jose Reyes-Gasga
Galo Cárdenas-Triviño

Germanium nanoparticles from solvated atoms: synthesis and characterization

Received: 17 March 2004
Accepted: 23 September 2004
Published online: 1 December 2004

R. A. Segura · G. Cárdenas-Triviño (✉)
Laboratorio de Atomos Metálicos,
Departamento de Polímeros,
Facultad de Ciencias Químicas,
Universidad de Concepción,
Casilla 160-C, Concepción, Chile
E-mail: gcardena@udec.cl
Tel.: +56-41-203337
Fax: +56-41-245974

J. Reyes-Gasga
Instituto de Física, UNAM,
Apartado Postal 20-363,
01000, Mexico D.F., Mexico

Abstract Germanium nanoparticles were synthesized by the chemical liquid deposition method (CLD) in which the Ge atoms, produced resistively, were co-deposited with 2-propanol, acetone and tetrahydrofurane vapors to obtain colloidal dispersions. The colloidal dispersions were characterized by UV-vis spectrophotometry, transmission electron microscopy (TEM), high resolution transmission electron microscopy (HRTEM), selected area electron diffraction (SAED) and Infrared Spectroscopy (FTIR) techniques. The Germanium colloids are, in general, kinetically unstable. Strong absorption bands in the UV region suggest that nanoparticles obtained by this procedure exhibit quantum confinement. In the Ge colloids, the particle size distribution is highly sensitive to concentration change. For example, the TEM measurements revealed for the Ge-2-propanol colloid, particle sizes close to 3 nm for a concentration of 10^{-3} M and 30 nm for a concentration of 10^{-2} M. The HRTEM and SAED showed the high crystallinity of the nanoparticles, and it was possible to observe the typical lattice spaces of a diamond cubic Ge structure. The FTIR studies revealed the Ge-organic nature of the particles surface. Mechanisms and structures have been proposed for surface reactions.

Keywords Ge nanoparticles · Nanostructures · Colloids · Colloid Stability · CLD · Quantum confinement

Introduction

The study of nanoparticles has become one of the most interesting areas in material science due to their unusual properties, different to the corresponding macro crystalline bulk material. These unique chemical and electronic properties have a potential use in the fields of non-linear optics, luminescence, electronics, optoelectronics and others [1–7].

The semiconductor nanoparticles also exhibit a change in their electronic properties relative to that of the bulk material. Electronic transport and optical excitations across the gap depend strongly on the size [8]. For example, when the particle size becomes smaller, the band gap becomes larger. This allows us to change the electronic properties of the material controlling the particle size [5]. The investigation on semiconductor nanoparticles, or quantum dots, is one of the most attractive areas in semiconductor science and technology [9]. A great interest in group IV nanoparticles stems from reports of efficient luminescence in these materials and the possibility of new materials for optoelectronic applications [10, 11]. The aim of this work is the synthesis and characterization of Ge nanoparticles. Several authors report a strong visible photoluminescence in Ge nanocrystals, which makes this system of very interesting [12–20].

There are several physical and chemical methods to prepare Ge nanoparticles. Some groups have used the rf-magnetron co-sputtering of Ge and SiO_2 onto Si substrates to produce thin films containing Ge nanoparticles with diameters between 1 and 14 nm embedded within a silica matrix [13–16]. Paine and co-workers prepared Ge/Si thin films on a Si substrate by CVD. A sequential hydrothermal oxidation, reduction by hydrogen and annealing at 700 °C produce Ge nanoparticles with diameters between 3 and 5 nm in a SiO_2 matrix [21, 22]. Another method to obtain nanoparticles involves the preparation of Ge colloids by ultrasonic mediated reduction of chlorogermanes and organochlorogermanes in an Na–K dispersion followed by a high pressure annealing at 270 °C [23]. They achieved the synthesis of Ge quantum dots with three different size distributions >20, 10 and 6 nm. Another method developed by Lukehart and co-workers consists in the addition of an organo germanium compound to a modified conventional sol–gel formulation, yielding a silica xerogel doped with this molecular species. A subsequent thermal treatment, under first oxidizing and then reducing conditions, affords Ge nanoclusters of 6.8 nm highly dispersed in the xerogel matrix [24]. The metathesis reaction of NaGe, KGe or Mg_2Ge with excess of $GeCl_4$ or $GeCl_2$ in glyme solvents described by Kauzlarich produces nano crystalline Ge with different alkyl surface terminations and average particle sizes between 3 and 10 nm [17, 18]. With this technique, Kauzlarich and co-workers have also prepared Ge/Si-R and Ge/SiO_2 core-shell nanostructures [19]. More recently, Kauzlarich and co-workers synthesized Ge nanoclusters of 4 nm with several functional groups like acetals, alcohols, esters and polymers attached [20].

All these techniques have some advantages and disadvantages. In some methods, a disadvantage consists in that the Ge nanoparticles are embedded in a matrix, which produces difficulties in the analysis; other techniques like CVD produce very small quantities of the desired material.

In this work, we are focused on the preparation of Ge nanoparticles by a non-traditional method. The chemical liquid deposition method (CLD), developed by Klabunde et al. [25], involves the resistive evaporation of metal and co-deposition with organic solvents at 77 K to obtain colloidal dispersions of metal-coated nanoparticles. The main difference with other methods is that Ge° clusters are obtained in one stage and no further reduction stages are necessary. By this method, it has been possible to obtain Pd, Au, Ag, Cd, and Zn monometallic dispersions, and Au–Pd, Au–Ag, Zn–Cd bimetallic dispersions [26–33]. The most important advantage of the CLD technique is that no by-products of metal salt reduction are present and pure metal colloids are formed. Another advantage consists in the control of the surface composition using different organic molecules for the covering. Furthermore, the material obtained is easy to handle for analysis. An additional improvement of the CLD technique consists in the synthesis of useful amounts of nanoparticles and the possibility of scaling up the process.

Experimental section

Synthesis of germanium colloids

Germanium colloids were prepared by the so-called chemical liquid deposition method (CLD), which involves the physical vapor deposition of metallic Ge in the presence of organic vapors. The reaction was carried out in a glass Metal Atom Reactor (Kontes). Typically, a W-Al_2O_3 crucible loaded with Ge was assembled in the glass reactor and the whole system was pumped off. A glass tube with the organic solvent (2-propanol, acetone, THF p.a. grade, purchased from Fisher), dried with molecular sieves and previously degasified three times by standard freeze-thaw procedure, was attached to a neck of the glass reactor. The whole system was immersed in liquid nitrogen (77 K) and evacuated to reach a vacuum of 10^{-5} bar. The crucible was heated using 30 A to reach the Ge boiling point. In the reaction, the Ge and the solvent were co-deposited over a period of half an hour. The frozen matrix, obtained in the walls of the reactor, was allowed to warm slowly over a period of one hour. Then, extra pure nitrogen gas was allowed to fill the reactor. After 30 min under nitrogen flow, a colloidal dispersion of Ge in organic medium was obtained. In a typical reaction, 7.3 mg (1×10^{-4} mol) of metallic Ge (purchased from Aldrich) was evaporated with 100 ml of dried and degassed 2-propanol to obtain the Ge-2-propanol 10^{-3} M colloid.

Characterization techniques

For the UV-vis study, 0.1 ml of the Ge-2-propanol colloid (1×10^{-3} mol/l) was diluted in 2-propanol (3 ml) to decrease the high absorption and prevent the particle agglomeration. The diluted colloid was placed in a rectangular quartz cell of 1 cm of optical path length and analyzed in a Spectronic Genesis 2 Spectrophotometer. A blank of pure 2-propanol was examined before every sample to eliminate solvent absorption. The UV-vis optical absorption spectra were recorded at room temperature at appropriate time intervals.

For the conventional transmission electron microscopy (TEM) and high resolution transmission electron microscopy (HRTEM) studies, a drop of Ge Colloid was dried on a carbon-coated Cu Grid (purchased from EMS). For the TEM, the samples were analyzed in a Jeol 1200 EX operating at 120 KeV of acceleration

voltage and with a point resolution of ~4 Å. For HRTEM measurements, a Jeol 4000 EX microscope, operated at 400 KeV and with a point resolution of ~1.7 Å, was employed. The pictures were taken at several magnifications. Selected area electron diffraction (SAED) was also performed in the samples with the HRTEM equipment.

FTIR was performed in a Nicolet Magna 5PC Spectrophotometer. The colloids were dried and the samples were prepared in a KBr pellet (~2% w/w). The spectra were carried out between 400 and 4,000 cm^{-1}, with an accumulation of 128 scans, collected and processed with the Omnic 5.2a software package.

Results and discussion

The reaction carried out by the method outlined in the experimental section produced Ge colloids at different molar concentrations and in different solvents, such as 2-propanol, acetone and THF. A general scheme of the reaction can be represented by Eq. 1, where L represents the organic solvent molecule. After condensation at 77 K, the solid Ge-organic matrix was warmed to obtain the colloid.

$$nGe^{0}(g) + xL(g) \xrightarrow{77K} Ge_nL_y(s) + L_{x-y}(s) \qquad [1]$$

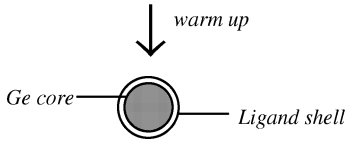

It was found that the stability of Ge colloids in the organic solvents employed have the following tendency: 2-propanol > acetone ≥ THF. For lower concentrations (10^{-3} M), after a fraction has flocculated, the Ge-2-propanol colloid reached a stability of several weeks, whereas the Ge-acetone and Ge-THF colloids floccules quickly before 48 h, even under nitrogen atmosphere. At higher concentrations (10^{-2} M), all colloids coagulate before 24 h due to the bigger particle size. Qualitatively, the colloids synthesized are transparent, but they turn whitish when the Ge particles are flocculating. The Ge colloids obtained by these methods are, in general, kinetically unstable. This instability is due to the high reactivity of Ge nanoparticles. In these particles, the motion is brought by the action of the Brownian motion and the rate of coagulation is largely controlled by the magnitude of the van der Waals interaction. The high reactivity is performed since nanoparticles have a great fraction of atoms localized on the surface. These surface atoms have low coordination states, making them more reactive than bulk Ge atoms. The Ge nanoparticles are also more reactive than metal noble nanoparticles. Then, the Ge nanoparticles react between them, growing and making the gravity effect stronger, and afterwards they coagulate. Another factor that affects the colloid stability is the contact with reactive atmospheres. For example, the contact with the wet air accelerates the flocculation process especially in particles with a deficient protective shell.

Figure 1 shows the absorption spectra of the Ge-2-propanol 1×10^{-3} M colloid, exposed to the air, in the 200–400 nm range recorded at different times. We can see a maximum close to 204 nm in which the absorption decreases quickly by time. In Fig. 2, a graphic of the peak absorbance as a function of time is shown. This tendency reveals a quick loss of the absorbance in the Ge-2-propanol colloid during the first 24 h. The Ge particles are flocculating and there is a smaller particle concentration each time. This produces a monotonous absorbance decay.

Quantum size effects have been experimentally observed on several nanocrystalline semiconductors [1, 3, 4, 8, 34, 35]. The optical absorption spectrum of a nanocrystalline semiconductor provides an available and straightforward method for the evaluation of quantum size effects. Experimentally, quantum size effects are observed as a shift toward higher energy values for the band edge (a blue shift), as compared to the typical value for the corresponding macrocrystalline material. Quantum confinement results in optical properties that are highly size-dependent, e.g., smaller nanoparticles absorb and emit light at higher energies than larger nanoparticles and have larger oscillator strengths. Such effects were clearly demonstrated in a study of CdS nanoparticles with different and well-defined particle size distributions [36]. In our case, while bulk Ge absorbs weakly in the infrared region, the Ge

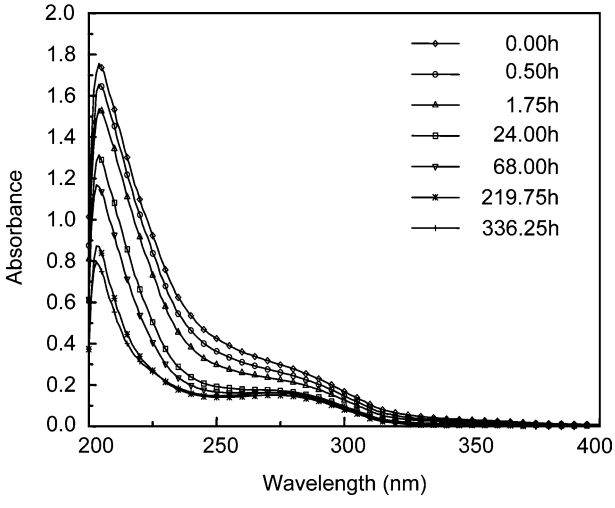

Fig. 1 The UV-vis absorption spectra of diluted Ge-2-propanol 10^{-3} M as a function of time

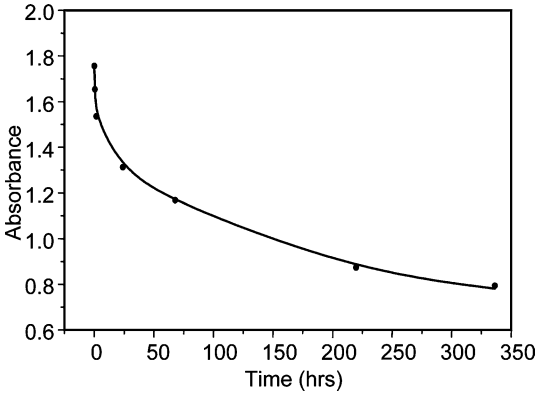

Fig. 2 Kinetic behavior of the 204 nm peak for the Ge-2-propanol 10^{-3} M colloid

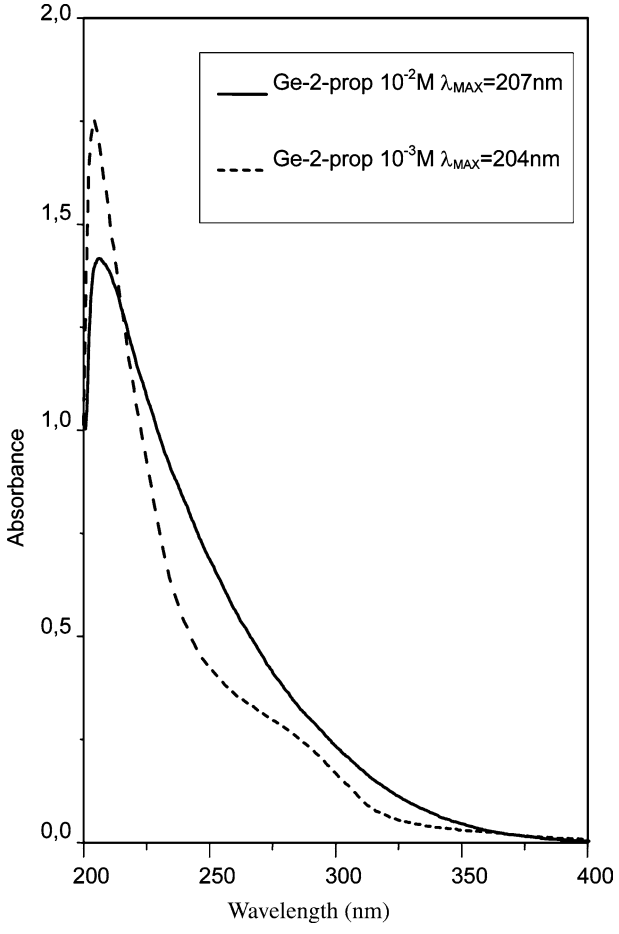

Fig. 3 The UV-vis absorption spectra of Ge-2-propanol 10^{-2} and 10^{-3} M fresh colloids

nanoparticles produced by the CLD method absorbs strongly in the ultraviolet region, near to 200 nm (see Figs. 1 and 3). This observation allows us to suggest that these Ge nanoparticles are probably quantum confined.

In Fig. 1 we can see a narrowing of the peak on the right side and an apparently slight shift in the maximum to higher energy as the time goes on. This narrowing of the bandwidth in the Ge-2-propanol 1×10^{-3} M colloid spectra means that when the flocculation process occurs the larger particles coagulate first, producing a narrowing in the size distribution. This fact allows us to suggest that the larger Ge particles are kinetically more unstable than smaller particles of the same system. For example, the Ge-2-propanol 1×10^{-2} M colloid is kinetically more unstable than the 1×10^{-3} M colloid, and absorbs at lower energy (207 nm); it is possible to expect that the particles have larger sizes. Figure 3 shows the spectrum for both Ge-2-propanol 1×10^{-2} M and 1×10^{-3} M fresh colloids, which exhibit a maximum (λ_{max}) at 207 and 204 nm, respectively. Moreover, the 1×10^{-2} M colloid have a broader absorption band as compared with the 1×10^{-3} M colloid, which indicates also a broader size distribution.

Another important fact in the absorption spectrum is the effect of the solvent. For both colloids synthesized in 2-propanol and THF (the acetone colloid cannot be studied due to instrument limitation), the initial optical spectra were similar and almost featureless. This indicates that the nanocrystalline core is mainly responsible for the absorption and that surface effects do not contribute significantly.

The nanoparticles were analyzed under the transmission electron microscope and the micrographs were taken at several magnifications. Making a statistical analysis, around 500 particles were measured in pictures on different places of the grid. The results were represented in a frequency Histogram (with Microcal Origin 4.00, Microcal Software Inc.) to obtain the particle size distribution. Figure 4 shows a typical TEM micrograph of a Ge-2-propanol colloid of 1×10^{-3} molar concentration. This micrograph reveals that the Ge particles have several particle sizes and the shape is predominantly spherical. The nanoparticles are randomly dispersed over the amorphous carbon support of the coated grid, and do not exhibit self-organizations. Figure 4 shows the particle size distribution found in the Ge-2-propanol 1×10^{-3} M colloid. The particle sizes are distributed mainly between 2 and 5 nm with an average particle size of 3 nm and a standard deviation of 0.7 nm. This size distribution is narrower than that obtained with other experimental methods of Ge-nanoparticle synthesis [13–15, 37]. This result makes the CLD synthesis of Ge nanoparticles more suitable to obtain materials for electronic purposes. CLD synthesis of Ge nanoparticles with other solvents, such as Acetone and THF, leads to similar particle size distributions (less than 10 nm for 10^{-3} M colloids) compared with the Ge-2-propanol ones. Although the size distribution is not largely sensitive to a solvent change, this is very sensitive to Ge-molar concentrations. For example, in the case of

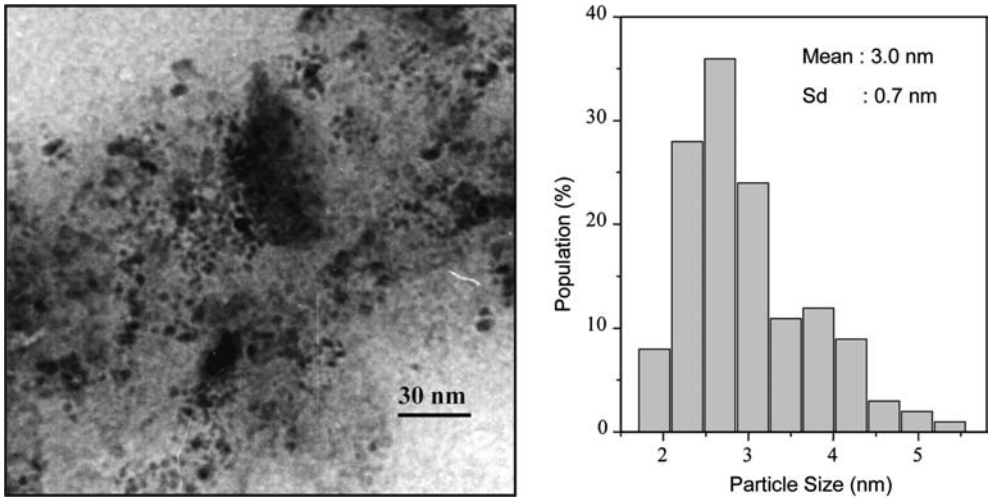

Fig. 4 The TEM micrograph and histogram of Ge-2-propanol 1×10^{-3} M colloid

Ge-2-propanol colloid, it is possible to obtain a size distribution around 3 nm for lower concentrations (1×10^{-3} M, 7.3 mg/100 ml), whereas at higher concentrations (1×10^{-2} M, 72.6 mg/100 ml), the particle size increases considerably with a distribution between 10 and 50 nm and an average of 30 nm (see Fig. 5 for the micrograph and the histogram).

This methodology is well reproduced if the conditions of evaporation rate, metal concentration and warm-up are kept constant [36].

To improve the visibility of the obtained HRTEM images, they were FFT filtered and reconstructed (with the Crisp 1.5f software, Calidris) to subtract the background generated by the grid support, and the noise produced during the image acquiring process. The HRTEM results revealed the high crystallinity of the Ge nanoparticles. Figure 6 shows a high resolution image of a Ge-2-propanol 1×10^{-3} M nanoparticle, where we can clearly discriminate that the atoms (white spots) are ordered in pseudo-hexagonal arrangements. The lattice spacings obtained from the picture are $d=2.02$ and 1.75 Å. These spacings, attributed to (220) and (311) lattice fringes, are typical of a diamond cubic Ge structure.

Selected area electron diffraction was performed in the samples with the Jeol 4000EX microscope. For Ge-2-propanol nanoparticles (10^{-3} M colloid), a rings pattern, shown in Fig. 7, was obtained. The rings in the diffraction picture were measured and then, the lattice spaces d_{hkl} (Å) $= K/D$ were calculated. $K=\lambda l$ is the microscope camera constant with a 2.8313 Å cm value for the microscope used (wavelength, λ, in angstroms by camera length, L, in centimeters). D corresponds to the ring diameter in centimeters. The lattice spaces d_{hkl} obtained (see Table 1) were compared with the crystallographic data of Ge (diamond cubic, tetragonal) and GeO_2 (orthorhombic, tetragonal, cubic, hexagonal) [38]. It was found that the crystallographic data is in agreement with a diamond cubic Ge structure, with an error smaller than 5% with respect to the reference data. These results

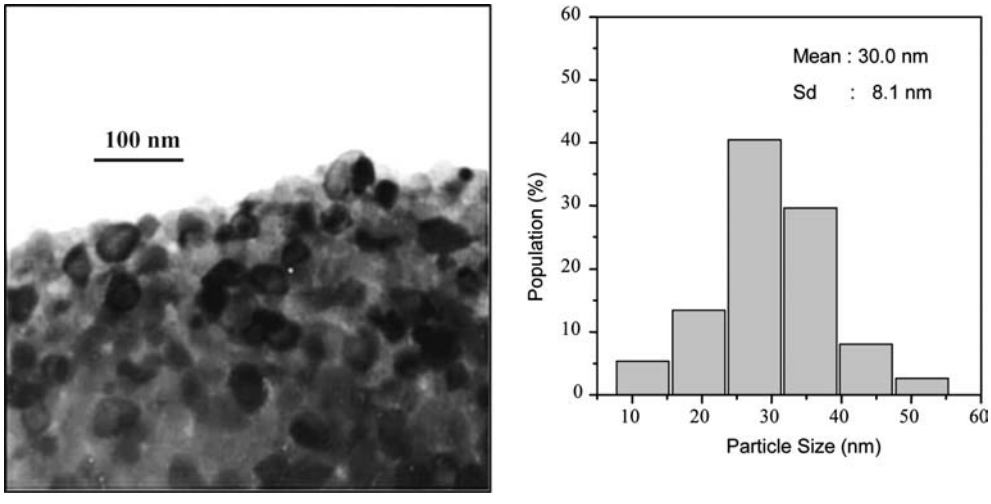

Fig. 5 The TEM micrograph and histogram of Ge-2-propanol 1×10^{-2} M colloid

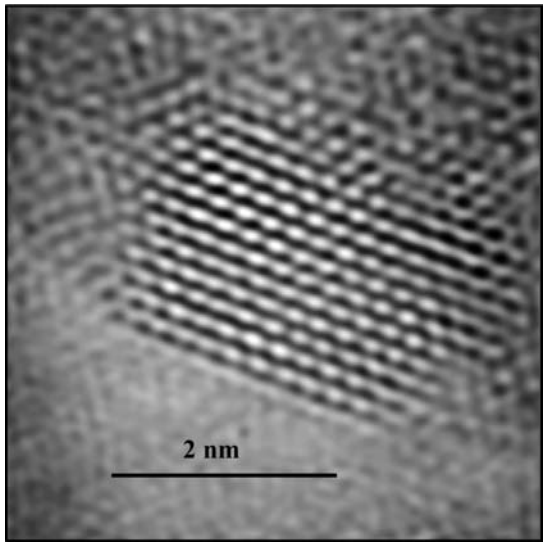

Fig. 6 The HRTEM micrograph of a Ge-2-propanol 10^{-3} M nanoparticle

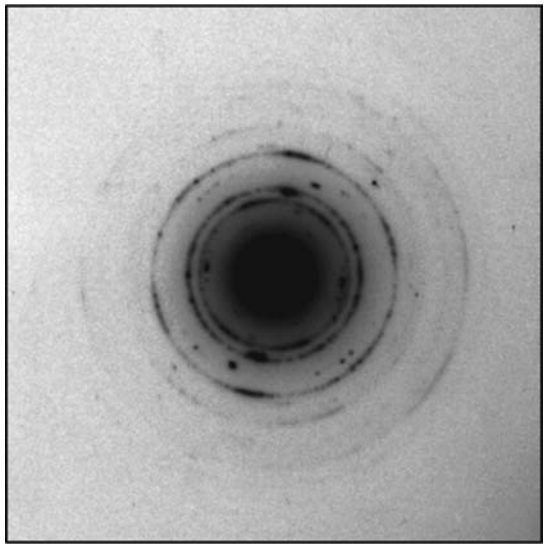

Fig. 7 Selected area electron diffraction pattern of Ge-2-propanol 10^{-3} M

Table 1 Lattice spaces, d_{hkl} exp, calculated from diffraction pattern of Ge-2-propanol 10^{-3} M. The error was calculated with respect to the reference crystallographic data, d_{hkl} ref, of Ge diamond cubic structure

D (cm)	d_{hkl} exp (Å)	d_{hkl} ref (Å)	Error (%)	*hkl*
1.451	1.951	2.000	2.45	2 2 0
1.789	1.583	1.633	3.06	2 2 2
2.025	1.398	1.414	1.13	4 0 0
2.295	1.234	1.298	4.93	3 3 1
2.666	1.062	1.089	2.48	3 3 3
2.936	0.964	0.956	0.84	5 3 1
3.274	0.865	0.863	0.23	5 3 3

are in agreement with the HRTEM results. Another information deduced from the rings pattern is that the crystallites (Ge nanoparticles) are randomly oriented over the carbon support and as a consequence rings appear in the diffraction pattern.

Another important aspect that must be resolved is the surface structure of the Ge-organic particles. For this purpose, FTIR was performed in the Ge nanoparticles synthesized with the different solvents: 2-propanol, acetone and THF. The FTIR spectra of the solids obtained from dried colloids are shown in Fig. 8. By comparison of the Ge colloids spectra with the pure organic solvents, we have clearly seen that new vibration modes appeared in the finger-print zone corresponding to organo-germanium modes. The spectra of Ge powders have also been compared with GeO_2 [39, 40], $(CH_3)_2Ge=CH_2$ [41], and Ge-tetraalkyls [42, 43]. It was found that the presence of Ge=C (near 860 and 810 cm^{-1}) and Ge–C (near 570 cm^{-1}) stretch vibrations, which in the 1,1-dimethyl-1-germene appear close to 850 and 820 cm^{-1} for the double bond and 570 cm^{-1} for single bond. These values are consistent with a previous work in which the FTIR and CIMS of Ge-acetone powders prepared by the same methodology were reported [44]. The presence of Ge=O bonds is almost discarded since such vibration should appear between 960 and 980 cm^{-1}.

With all the previous evidences, we can postulate possible structures of the manner in which the molecules are inserted in the Ge surface. For example, the reaction mechanism of acetone over a Ge (100) surface has recently been reported in the literature [45]. In that work,

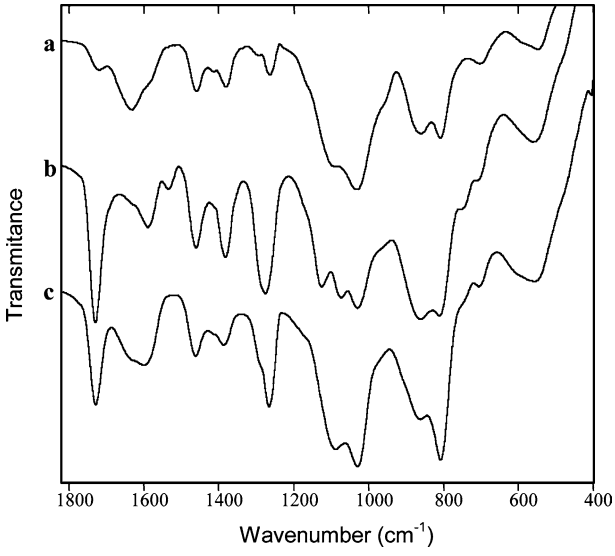

Fig. 8 The FTIR spectra of dried Ge colloids. Spectra *a*, *b*, *c* correspond to Ge-2-propanol, Ge-acetone and Ge-THF colloids (10^{-3} M), respectively

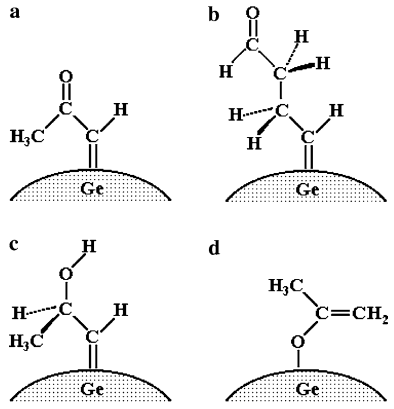

Scheme 1 Proposed superficial structure for Ge nanoparticles. The **a** adduct corresponds to Ge-acetone, the **b** adduct corresponds to Ge-THF, and the **c** and **d** correspond to Ge-2-propanol

the authors propose, according to FTIR evidence, that acetone undergoes attachment at the carbonyl oxygen with the loss of an α hydrogen on the Ge (100) surface to form an enol-like adduct. They detect in the FTIR spectrum the loss of the C=O band (1,710 cm^{-1}), and the formation of a new band at 1,640 cm^{-1} corresponding to a C=C bond. In our case, with the synthesis of Ge-acetone colloid there is no loss of the carbonyl band, but there is formation of germanium–carbon bonds. We postulate that Ge reacts with a Cα of the acetone, forming Ge–C bonds (single and/or double), as can be seen on Scheme 1. The bands for pure acetone are *ν*C=O at 1,715 cm^{-1} and *ν*C-O at 1,092 cm^{-1}. For the Ge-2-propanol colloids, two mechanisms seem to be involved, since the presence of Ge=C and C=C bonds is detected. For this case, we propose two possible kinds of adducts (see Scheme 1c, d). In Scheme 1c, Ge would be reacting with a primary carbon of the 2-propanol to form an adduct similar to the acetone (Scheme 1a) but with an O–H group instead of a C=O group. The other possible Ge-propanol adduct would be the one when Ge reacts with the 2-propanol oxygen; this is supported by the evidence of a C=C band at 1,630 cm^{-1}. This adduct is the same proposed for the acetone Ge (100) surface reaction. For the Ge-THF reaction, we propose that Ge reacts with a carbon adjacent to the oxygen of the THF, causing a ring opening and a subsequent formation of a C=O bond supported by the presence of a band close to 1,729 cm^{-1}, and the absence of the C–O stretching. The adduct structure is presented in Scheme 1b. All mechanisms and structures proposed for the anchoring of the organic molecules over the Ge surface are tentative and need further studies. A relationship between colloidal stability and the FTIR studies can be carried out to conclude that the stability is a consequence of the proposed adducts in the Ge surfaces. The Ge-2-propanol adduct with the superficial O–H group could provide a more efficient protective shell, forming hydrogen bridges with the 2-propanol and due to this fact the Ge-2-propanol colloid is the most stable.

Conclusions

The CLD synthesis allows us to obtain successfully Ge-2-propanol, Ge-acetone and Ge-THF colloids in a range of Ge/solvent concentrations between 10^{-3} and 10^{-2} M (mol/l). The UV spectroscopy shows that Ge colloids are kinetically unstable. The UV results also show that the nanoparticles absorb strongly in the 200–220 nm region; this is an evidence that supports their quantum confinement. The particle size distribution depends on the initial colloid concentration and increases drastically from 3 nm to about 30 nm in average for Ge-2-propanol when the concentration increases from 10^{-3} to 10^{-2} M. These results are consistent with UV-absorption bands. For colloids with broader size distributions, the UV absorption are also broader when compared with narrow size distribution colloids. The HRTEM results for Pd-2-propanol 1×10^{-3} M show the high crystallinity of the Ge nanoparticles, and the electron diffraction confirms that we are in the presence of zerovalent Ge instead of Ge oxide. The FTIR study reveals the Ge-organic vibration interactions, allowing us to suggest a tentative mechanism of how the organic fragments are anchored in the Ge surface. Finally, it is important to remark that this synthesis yields Ge nanoparticles in useful amounts and it is very suitable for the design of tailored semiconductor nanoparticles with potential electronic applications, being able to control partially the particle size ranges and their surface composition.

Acknowledgements This contribution was possible thanks to the financial support of Fondecyt (Grant 2010108), CONICYT for the Ph.D. Fellowship, and Mecesup UCO9905. The authors wish to thank Dirección de Investigación, Universidad de Concepción particularly Mr. Raúl Alarcón of the TEM laboratory. The authors also wish to thank Mr. Luis Rendón, Ms. Cristina Zorrilla, Mr. Samuel Tehuacanero, Mr. Pedro Mexia, and Mr. Roberto Hernandez of HRTEM and Image Processing Laboratory of the Instituto de Física de la UNAM, México.

References

1. Henglein A (1989) Chem Rev 89:1861
2. Schmid G (1992) Chem Rev 92:1704
3. Steigerwald ML, Brus LE (1990) Acc Chem Res 23:183
4. Fendler JH, Meldrum FC (1995) Adv Mater 7:607
5. Trindade T, O'Brien P, Pickett NL (2001) Chem Mater 13:3843
6. Schmid GJ (1998) Chem Soc Dalton Trans 1077
7. Yacamán MJ, Mehl RF (1998) Metal Mater Trans A 29A:713
8. Alivisatos APJ (1996) Phys Chem 100:13226
9. Huang J, Ye Z, Wang LJ (2002) Mater Sci Lett 21:129
10. Brus LEJ (1994) Phys Chem 98:3575
11. Sailor MJ, Kavanagh KL (1992) Adv Mater 4:432
12. Wu XL, Siu GG, Gu Y, Tang N, Gao T, Bao XM (1999) Appl Phys Lett 74:827
13. Kanemitsu Y, Uto H, Masumoto Y, Maeda Y (1992) Appl Phys Lett 61:2187
14. Maeda Y, Tsukamoto N, Yazawa Y, Kanemitsu Y, Masumoto Y (1991) Appl Phys Lett 59:3168
15. Fujii M, Hayashi S, Yamamoto K (1990) Appl Phys Lett 57:2692
16. Takeoka S, Fujii M, Hayashi S, Yamamoto K (1998) Phys Rev B 58:7921
17. Taylor BR, Kauzlarich SM, Delgado GR, Lee HW (1999) Chem Mater 11:2493
18. Taylor BR, Kauzlarich SM, Lee HW, Delgado GR (1998) Chem Mater 10:22
19. Yang CS, Kauzlarich SM, Wang YC (1999) Chem Mater 11:3666
20. Tanke RS, Kauzlarich SM, Patten TE, Pettigrew KA, Murphy DL, Thompson ME, Lee HW (2003) Chem Mater 15:1682
21. Paine DC, Caragianis C, Kim TY, Shigesato Y, Ishahara T (1993) Appl Phys Lett 62:2842
22. Paine DC, Kim TY, Caragianis C, Shigesato YJ (1994) Electron Mater 23:901
23 Heath JR, Shiang JJ, Alivisatos APJ (1994) Chem Phys 101:1607
24. Carpenter JP, Lukehart CM, Henderson DO, Mu R, Jones BD, Glosser R, Stock SR, Wittig JE, Zhu JG (1996) Chem Mater 8:1268
25. Klabunde KJ, Timms PL, Skell PS, Ittel S (1979) Inorg Synth 19:59
26 Cárdenas-Triviño G, Klabunde KJ, Dale EB (1987) Langmuir 3:986
27 Lin S, Franklin MT, Klabunde KJ (1986) Langmuir 2:259
28. Cárdenas-Triviño G, Vera V, Muñoz C (1998) Mater Res Bull 33:645
29. Cárdenas G, Ponce A (1996) Colloid Polym Sci 274:788
30. Cárdenas G, Oliva C, Carbacho H (1995) Bol Soc Chil Quim 40:261
31. Cárdenas G, Segura R (2000) Mater Res Bull 35:1369
32. Cárdenas G, Segura R, Morales J, Soto H, Lima CA (2000) Mater Res Bull 35:1251
33. Cárdenas G, Segura R, Morales J, Soto H, Lima CA (2000) Polyhedron 19:2337
34. Weller H. (1993) Angew Chem Int Ed Engl 32:41
35. Hagfeldt A, Grätzel M (1995) Chem Rev 95:49
36. Klabunde KJ, Cárdenas-Triviño G (1996) Metal atom/vapor approaches to active metal cluster/particles. VCH, New York, p 237
37. Vossmeyer T, Katsikas L, Giersig M, Popovic IG, Diesner K, Chemseddine A, Eychmüller A, Weller HJ (1994) Phys Chem 98:7665
38. Tomiya S, Petroff PM, Margolese D, Srdanov VY, Stucky GD, Zhang YH (1993) Mater Res Soc Symp 286:353
39. Powder Diffraction File, Inorganic Phases, JCPDS (1997) International Centre for Diffraction Data, Pennsylvania
40. Hassanzadeh P, Andrews LJ (1992) Phys Chem 96:6181
41. Withnall R, Andrews LJ (1990) Phys Chem 94:2351
42 Khabashesku VN, Kudin NK, Tamás J, Boganov SE, Margrave JL, Nefedov OM (1998) J Am Chem Soc 120:5005
43. Fuchs R, Moore L, Miles D, Gilman H (1956) J Org Chem 21:1113
44. Lippincott ER, Tobin MC (1953) J Am Chem Soc 75:4141
45. Cárdenas-Triviño G, Alvial JA, Klabunde K (1990)J Bol Soc Chil Quim 35:227
46. Wang GT, Mui C, Margrave CB, Bent SF (2001) J Phys Chem B 105:12559